CHAPTER 4

RESULT & DISCUSSION

4.0 Introduction

In order to present the experimental results of this work in a systematic fashion, this chapter has been divided into two main sections. The first section is analysis of the special structure A. The following section will be on the analysis of the special structure B. All the analysis is based on the graph generated from the data taken from the TSUPREM 4.

The graph to be discussed in the discussion are boron concentration for 120keV (without BF_2), boron concentration before and after diffusion (with BF_2), interstitial concentration before and after diffusion, vacancy concentration after diffusion, cluster concentration after diffusion, interstitial & vacancy concentration for BF_2^+ at 20kev, 35kev and 50kev for both structures A and B.

4.1 Effect Of Fluorine Implantation At The Surface After Boron Implantation In The Silicon Bulk

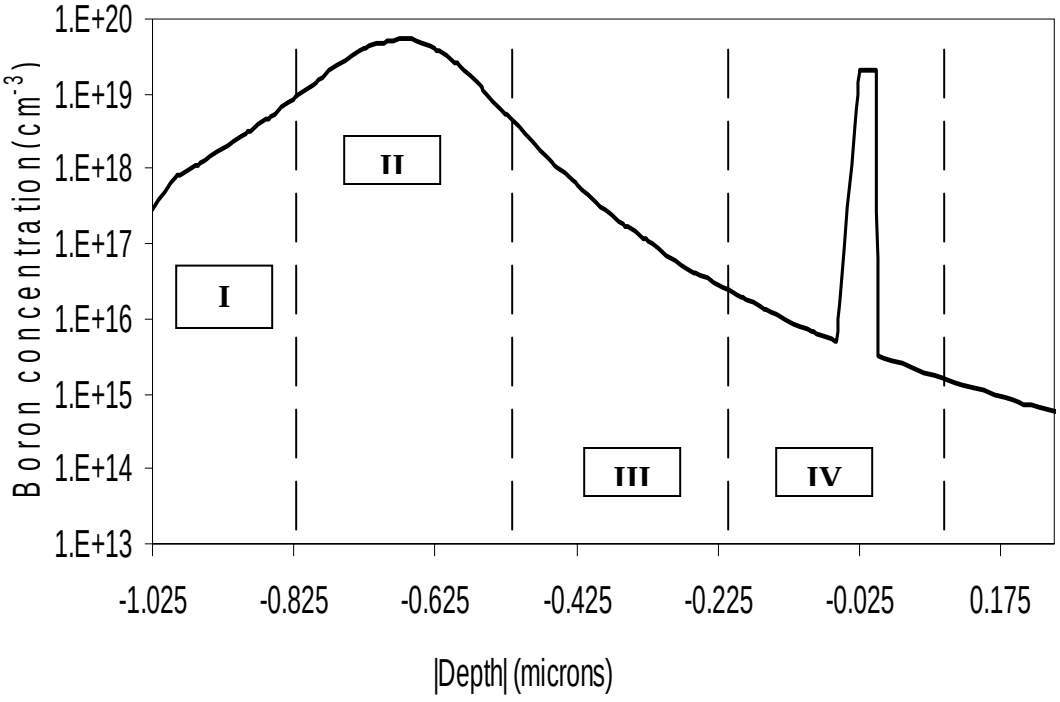

Figure 4.0: Boron concentration for 120keV boron implantation energy at the dose of $2 \times 10^{19}/cm^3$ without diffusion

In the initial stage, boron is implanted in the silicon bulk at 120 kev. Before BF_2^+ implantation is done at the surface, an understanding of boron diffusion in silicon is important. Figure 4.0 shows the boron concentration in silicon bulk and no diffusion process is performed. This figure is divided into 4 regions as show above. The surface region is represented by region I, the boron peak (bulk) region is represented by region II. The interface between boron and underlying layer is represented by region III and the underlying layer is represented by region IV. As boron implanted into the silicon bulk, boron atoms collided with the silicon atoms in the lattice that performed the kick-out mechanisms caused vacancies to occur at the surface [3]. The vacancies cause boron

concentration in the region I (surface) to be lower than the concentration of boron in region II (boron peak). It is because the surface area had ion implantation process and the energetic dopant ion bombardment damages the single-crystal structure of the silicon substrate. In the surface region, when the implanted ion collide with nuclei of the atoms are scatter significantly by the collision and transfer energy to the lattice atoms. In this 'hard' collision atoms can get enough energy to break free from the lattice binding energy, which causes crystal structure disorder and damage.

At the boron peak region (region II), the boron concentration and interstitial is high, it is because when the ion implantation process is done, the boron atom collided with the silicon atom in the lattice and created boron and silicon interstitial in the deeper area since vacancies are dominating at the surface (region I). The high concentration of boron in region II actually caused by the high concentration of boron interstitial created during ion implantation.

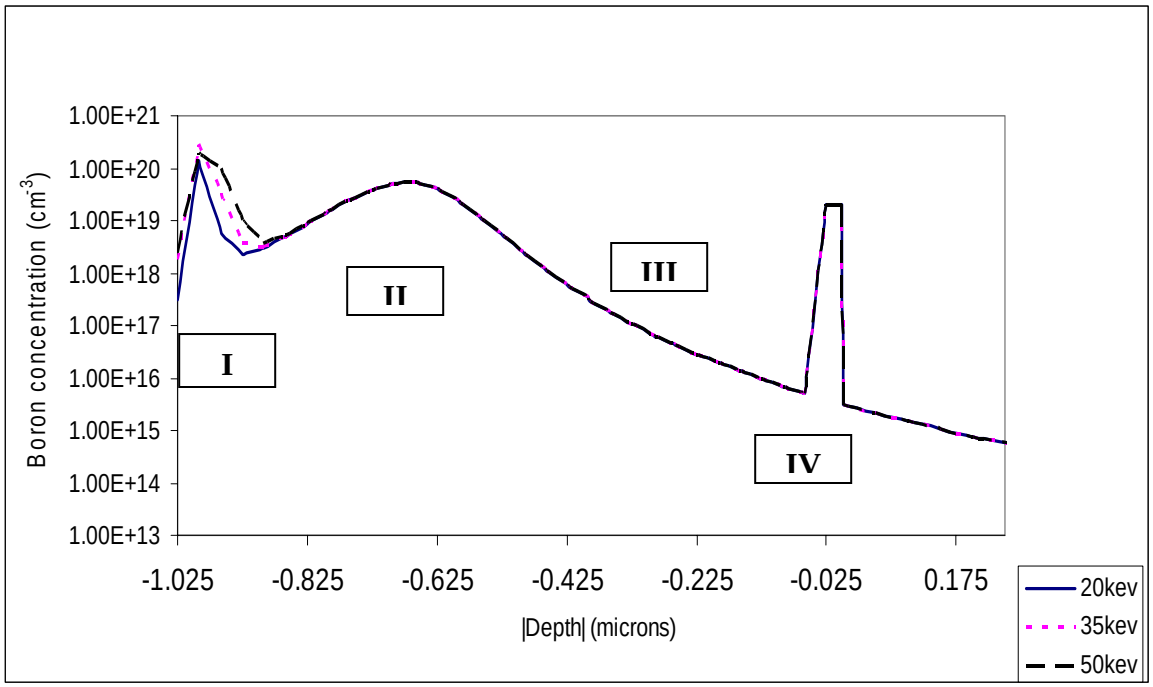

Figure 4.1: Different boron concentration of 120 keV boron implant followed by 20 keV, 35 keV and 50 keV BF_2^+ implantation before diffusion

Figure 4.1 shows the boron concentration for three different implantation of energies fluorine implanted to the structure. In the region I, it is seen that the boron concentration is higher than the region II. It is because the surface has became a vacancy rich area before BF_2^+ is implanted at the surface show in figure 4.0. Therefore, after BF_2^+ implantation, the vacancies at the surface after boron implantation had been filled with BF_2^+.

At region II, the boron concentrations for the three BF2+ implantation are the same. It is because before the BF_2^+ implantation, the region II is already filled with high concentration of interstitials so called interstitial rich region. Therefore the boron from BF_2^+ implantation cannot move to the deeper area. The region III and region IV are not activated and the implantation dopant atoms stopped at region II which caused by the ion stopping mechanisms [3].

From the graph in figure 4.1, it is observed that the higher the BF_2^+ implantation energy at the surface, the higher the boron concentration at the surface. Generally, the higher the ion energy, the deeper it can penetrate into the substrate. However, even with the same implantation energy, ion does not stop exactly at the same depth in the substrate, because each ion has different collisions with different atoms [3].

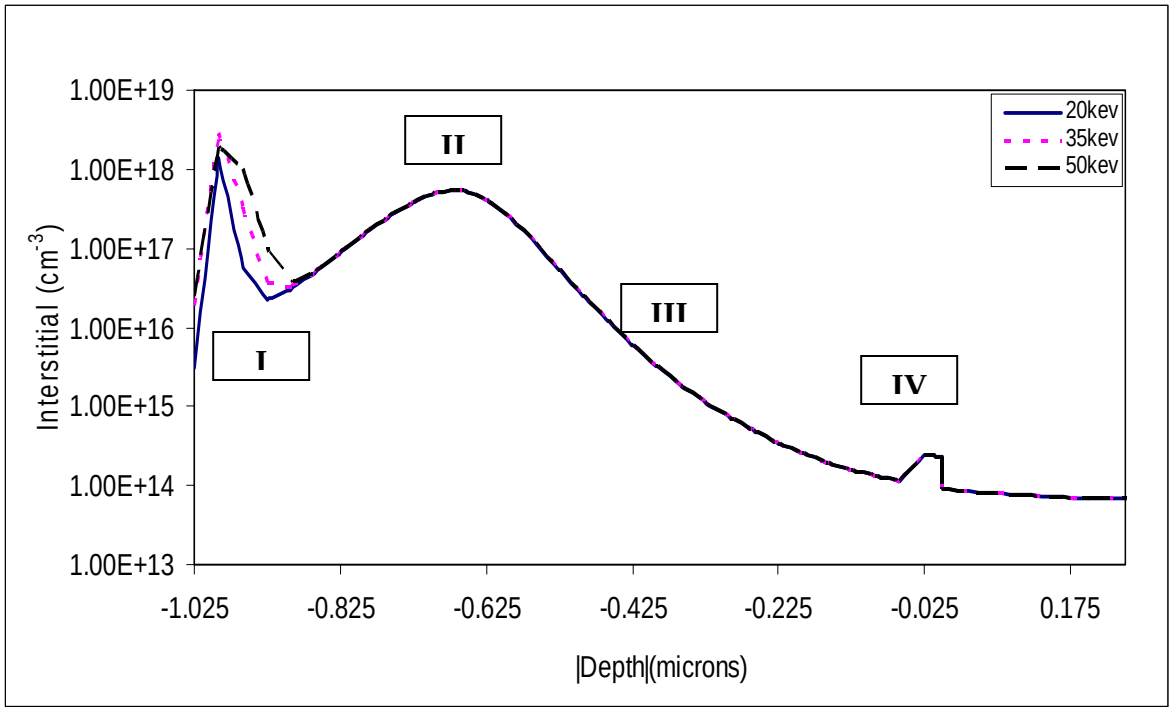

Figure 4.2: Different boron interstitial concentration for 120 keV implanted boron, dose of 2 x 10^{19}/cm^3 followed by 20, 35 and 50 keV BF_2^+ implantation before diffusion.

As discussed and explained in figure 4.1, the surface or region I has high peak of interstitial concentration around $\pm 1e18/cm^3$ because the atom B^+ have fit into the silicon lattice during the BF_2^+ implantation process. In the graph, it is shown that region IV also have some boron interstitial concentration, it is because the underlying layer had been deposited with boron before the BF_2^+implantation.

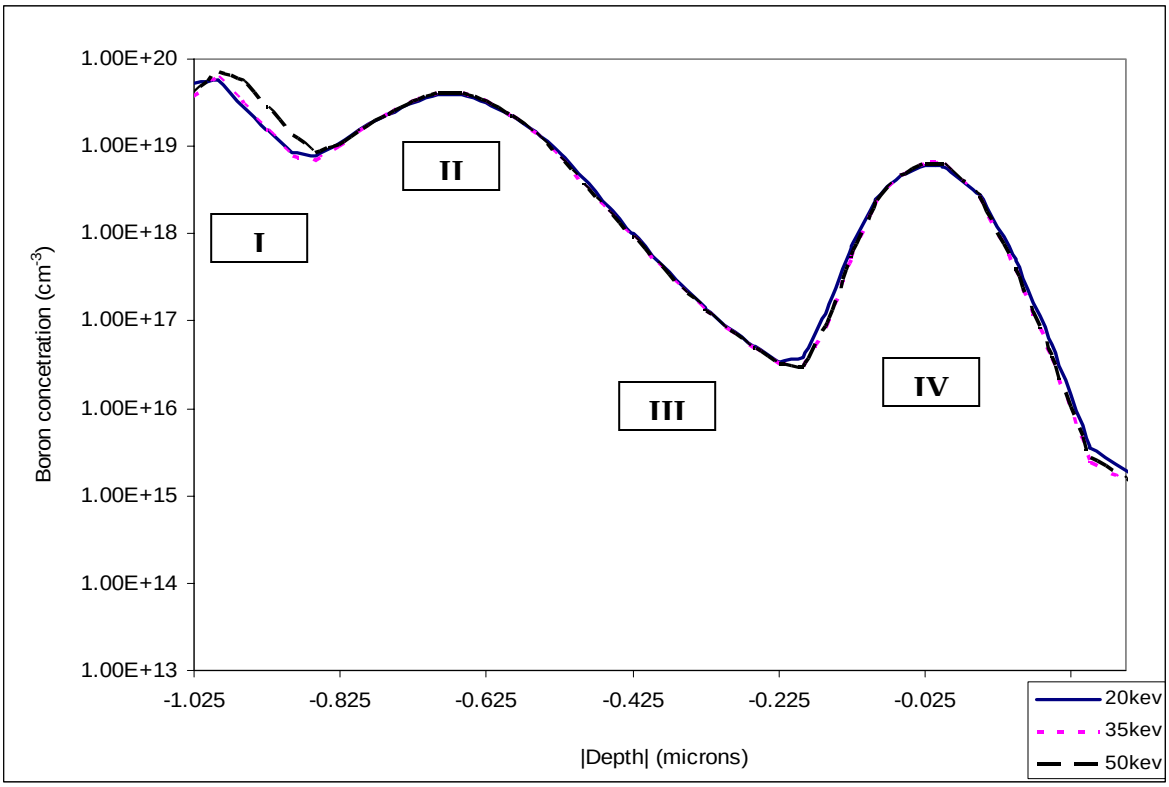

Figure 4.3: Different boron concentration of 120 keV implanted boron followed by 20 keV, 35 keV and 50 keV BF_2^+ implantation after diffusion.

To achieve a well operated device requirement, the lattice damage must be repaired in an annealing process to restore the single crystal structure and activate the dopant. Only when dopant atoms are at the single crystal lattices can they effectively provide electrons or holes as the majority carriers for electric current [3]. In high temperature process, atoms get energy from the heat and start rapid thermal motion. When they find the sites with the lowest free energy, which are located at single crystal lattices, they stay there. Since the undamaged substrate underneath is single crystal silicon, the silicon and dopant atoms in the damaged amorphous layer reconstruct the single crystal structure there by falling into the lattice grids and being bonded by the lattice energy [3].

Figure 4.3 shows that, the interstitial sinked at the surface region caused by the interaction with fluorine. It is because the presented of the fluorine act as sinks for interstitial boron [17]. When the annealing process is performed, the dopant will be

activated; the boron interstitials had enough energy and started to move forward to the region II. The boron atom in region II gain enough energy and also move forward to region III. The boron atoms in region therefore move forward to the region IV. As the result, the boron interstitial in the underlying layer is increased cause by the initial movement of boron atoms from the surface. By comparing the boron concentration at the surface before and after diffusion, the boron concentration peak before diffusion at the surface is higher. It is because the annealing activates the dopant, repair the lattice damage, and hence cause the loading of boron profile in the underlying layer.

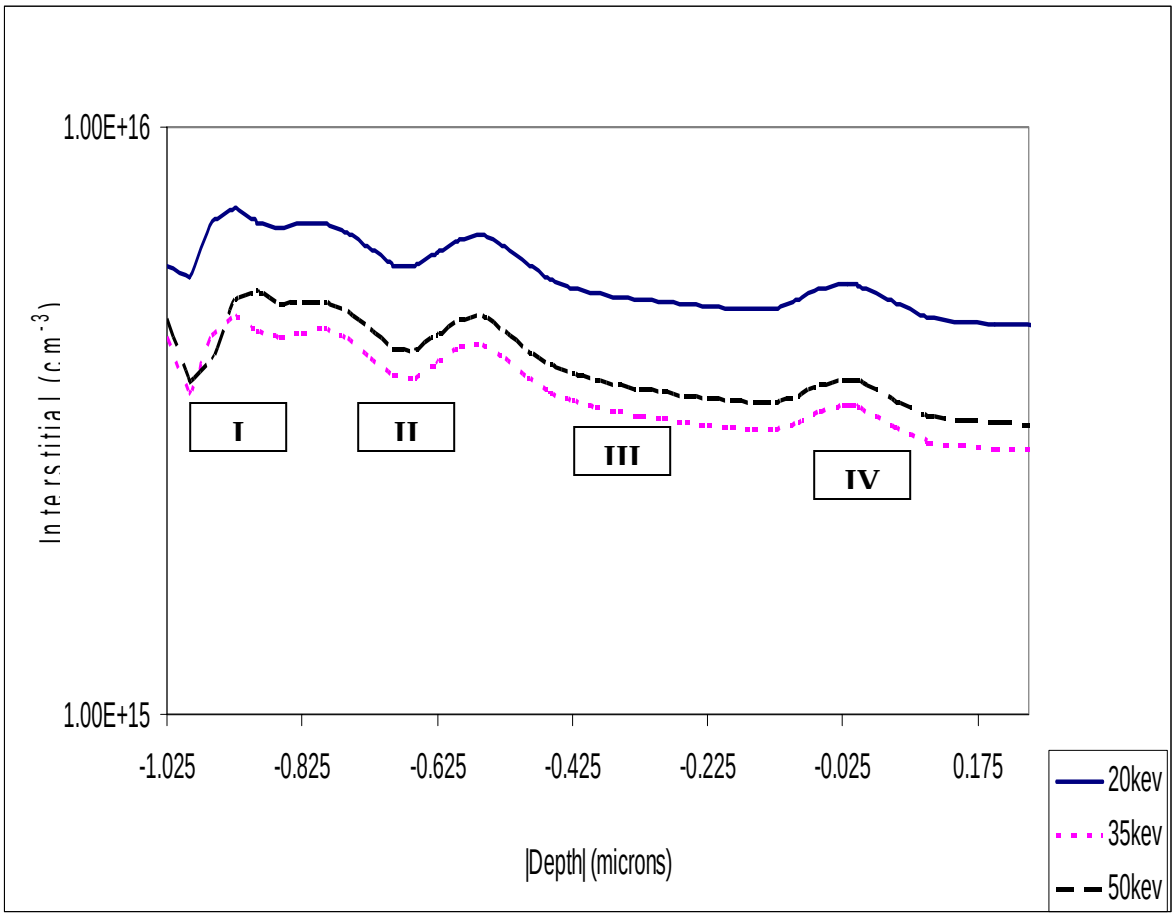

Figure 4.4: Different boron interstitial concentration for 120 keV implanted boron, dose of 2 x 10^{19}/cm^3 followed by 20, 35 and 50 keV BF_2^+ implantation after diffusion

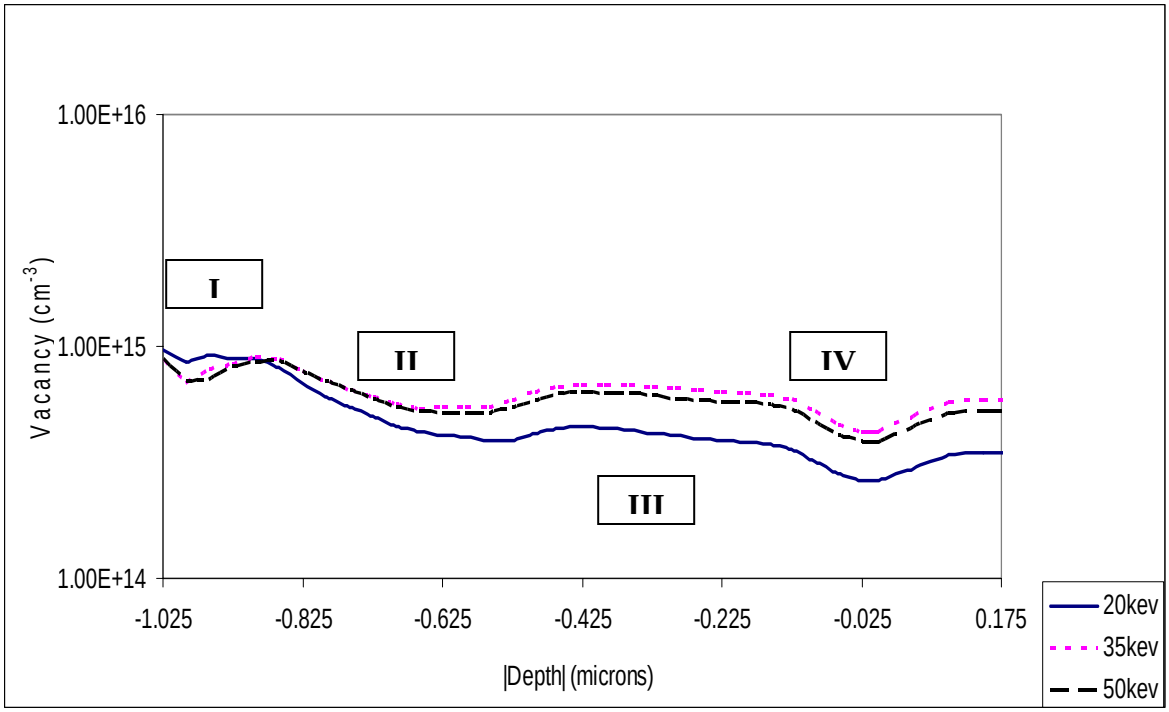

Figure 4.5: Different vacancy concentration for 120 keV implanted boron, dose of 2 x 10^{19}/cm^3 followed by 20, 35 and 50 keV BF_2^+ implantation after diffusion

Figure 4.4 and 4.5 shows the interstitials and vacancies concentration for three different BF_2^+ implantation energy of 20, 35 and 50 keV after diffusion. As show in figure 4.4, the interstitials at the region I are obviously lower compared to region I before diffusion as discussed in figure 4.2. this is because the atom boron at the surface received enough energy to move forward into the region II during the annealing process and fit into the lattice. The underlying layer also have been affect after the annealing process when the boron atom in the underlying layer have enough energy to move forward and fit into the vacancies in the silicon lattice.

From the figure 4.4, it is shown that the 20 keV BF_2^+ implanted have the higher interstitial concentration followed by 50 keV and 35keV. Generally, the higher the ion energy, the deeper it can penetrate inside the substrate. Therefore, the higher the implantation energy, the higher the concentration of the interstitial [3]. In this experiment, the used of the boron implantation energy is the same 120 keV. The differences are in the BF_2^+ implantation energies of 20, 35 and 50 keV. If fluorine was simply reduced boron

TED by interacting with the silicon interstitial, it is be expected that the increase in the BF_2^+ implantation energy would result in further reduction of the boron TED in the underlying layer.

In figure 4.5, it is observe red that the underlying layer at the region IV has lower vacancies concentration compared with the other region. It is because the vacancies in the underlying layer have been filled up by the boron atoms during the annealing process. In high temperature, atoms received energy from the heat and started to have rapid thermal motion.

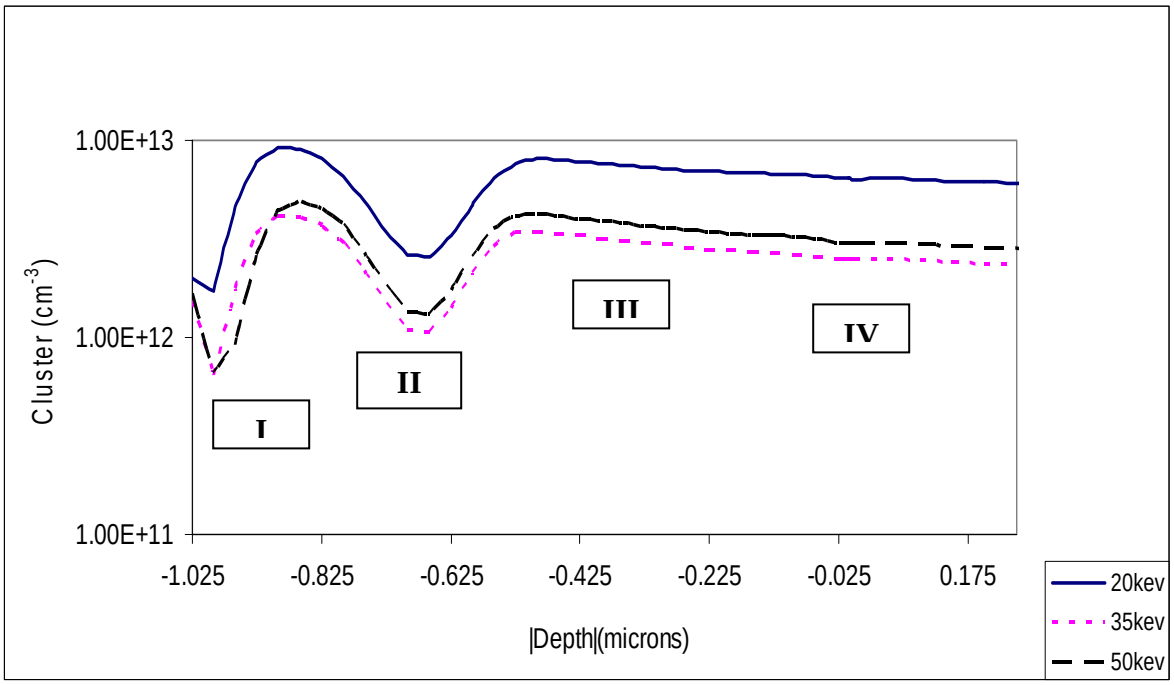

Figure 4.6: Different boron cluster concentration for 120 keV implanted boron, dose of 2 x $10^{19}/cm^3$ followed by 20, 35 and 50 keV BF_2^+ implantation after diffusion

In figure 4.6, the peak of boron cluster concentration for 20, 35 and 50 keV BF_2^+ are high in the bulk region at the depth of 0.825 microns and 0.425 microns. As shown in figure 4.2, the peak of interstitials concentration at the region II are the high (1E18 cm^{-3}), therefore during the annealing process, the atom inside the silicon lattice started to pair and

bonded together. The bulk region has higher cluster concentration due to the high concentration of boron in the bulk. The region III and region IV also have high cluster concentration because it has high boron interstitial concentration as shown in figure 4.4.

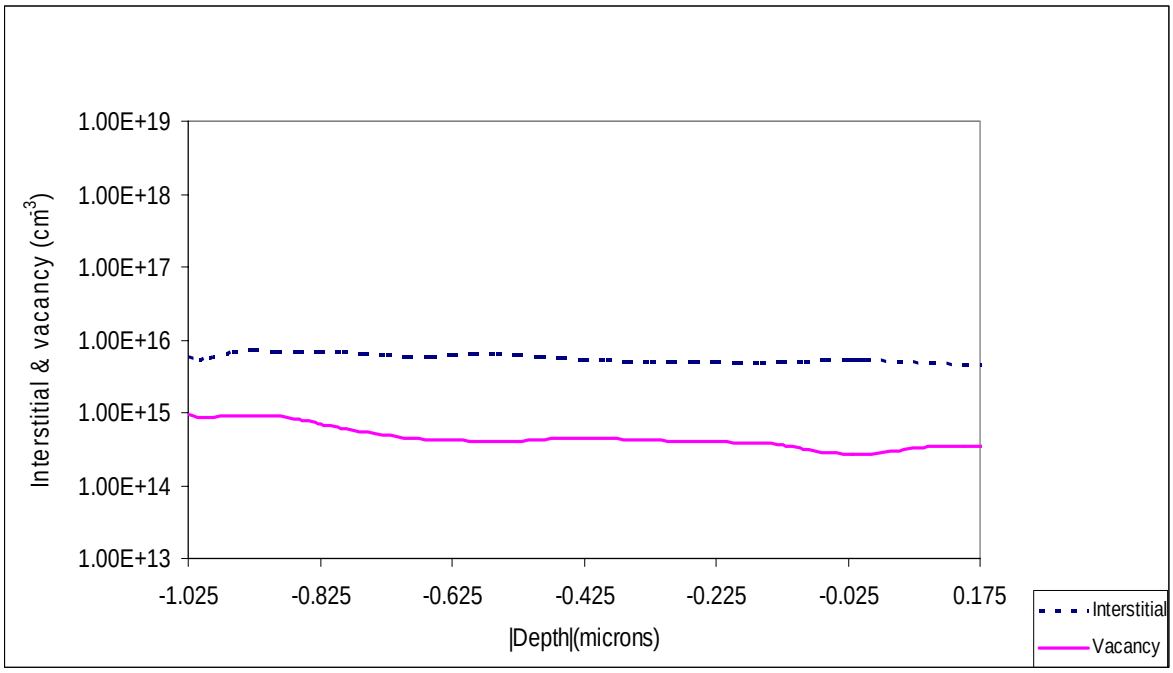

Figure 4.7: Interstitial and vacancy concentration for 120 keV implanted boron, dose of 2 x $10^{19}/cm^3$ followed by 20 keV BF_2^+ implantation after diffusion

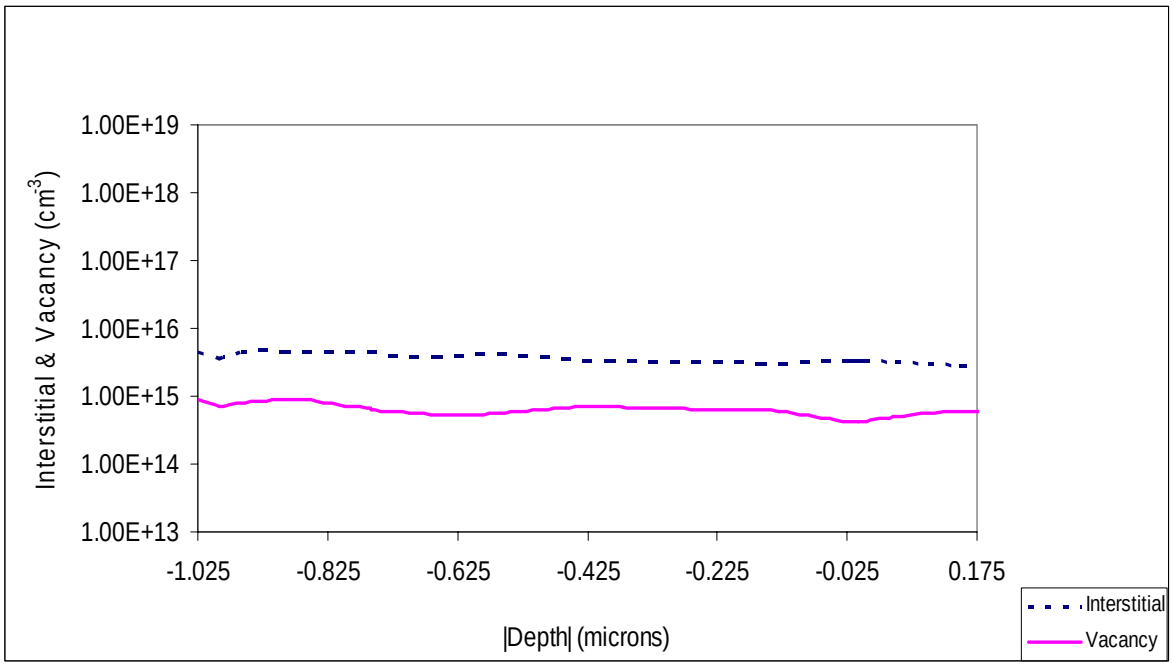

Figure 4.8: Interstitial and vacancy concentration for 120 keV implanted boron, dose of 2 x 10^{19}/cm^3 followed by 35 keV BF_2^+ implantation after diffusion

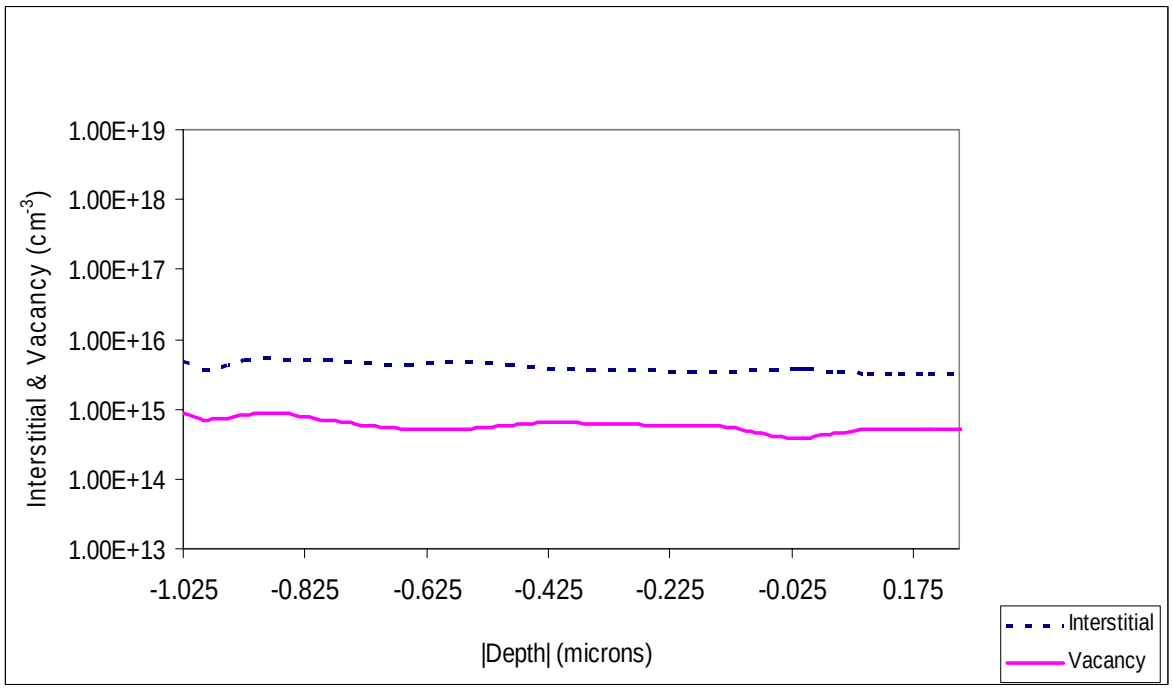

Figure 4.9: Interstitial and vacancy concentration for 120 keV implanted boron, dose of 2 x 10^{19}/cm^3 followed by 50 keV BF_2^+ implantation after diffusion

Figure 4.7, 4.8 and 4.9 shows the comparison of the interstitials and vacancies concentration for each of 20, 35 and 50 keV BF_2^+ implantation after diffusion. The results of the three figures show that the interstitials concentrations are between 1.00E+15 to 1.00E+16. The vacancies concentrations are between 1.00E+14 to 1.00E+15. It is observed that the interstitials concentrations profiles from the three figures are higher than the vacancies concentration.

4.2 Evolution Of Boron Diffusion.

Figure 4.10 shows the evolution of boron diffusion during annealing. In the graph, it shows that the transient enhanced diffusion at the underlying layer occurred between 0.05 second and 1 second. The width shows in the graph is the transient enhanced diffusion for the structure after diffusion. The width of underlying layer after 10second of annealing shows that the boron profile bonding in underlying layer between 10 second and 30 second has a small change compared to between 0.05 second to 1 second.

Form the graph, it is observed that at the surface and bulk regions (region I and region II) the peak of boron concentration is increasing with the increasing of the time of annealing. It is caused by the activation of boron atom and the interstitial sinking process during the annealing.

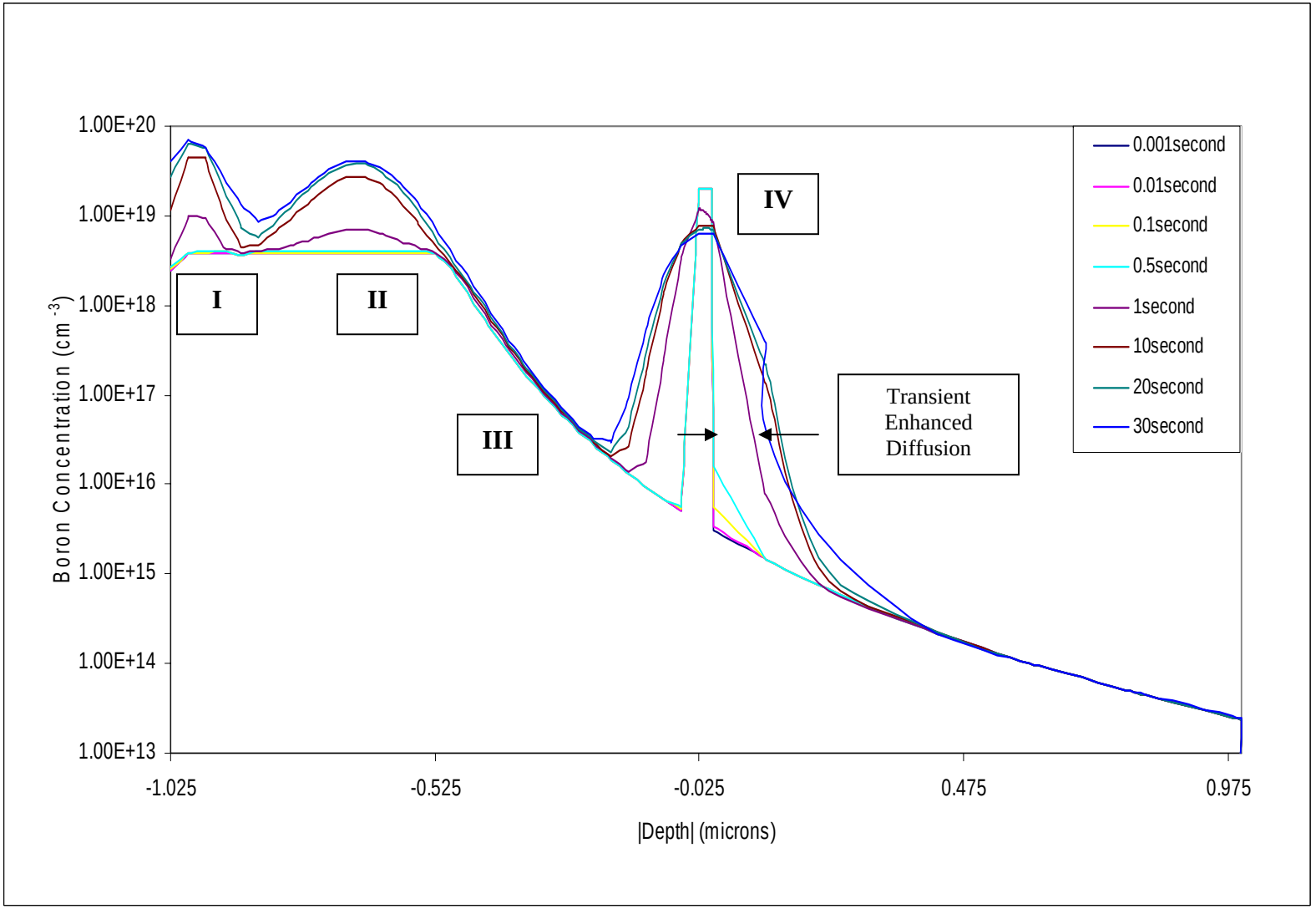

Figure 4.10: Boron concentration for 120 keV boron and 50 kev BF_2^+ implantation at the dose of 2 x $10^{19}/cm^3$ diffused at 900^oC with different annealing time

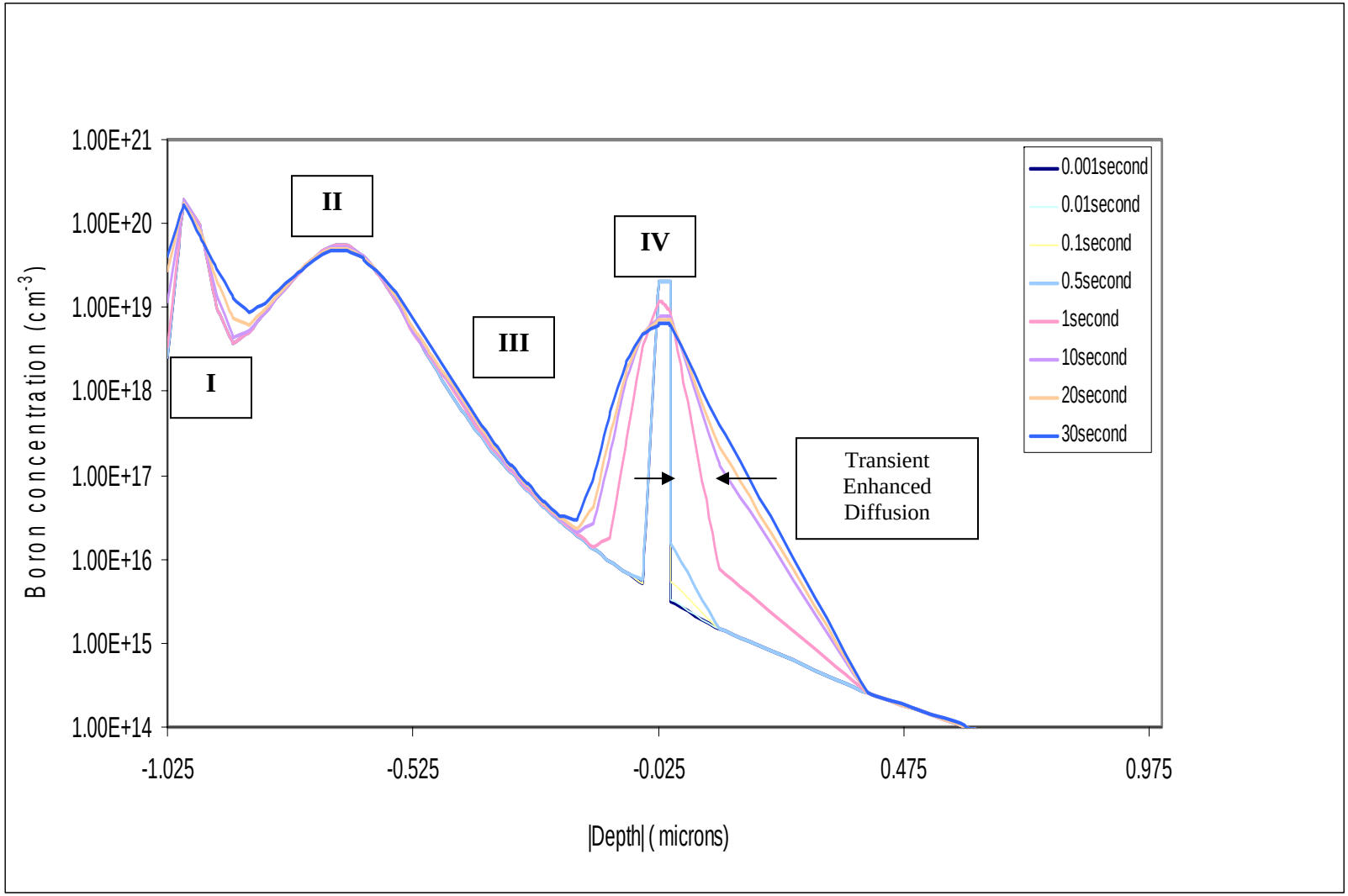

Figure 4.11: Boron active concentration for 120 keV boron and 50 kev BF_2^+ implantation at the dose of 2 x $10^{19}/cm^3$ diffused at 900^oC with different annealing time

4.3 Fluorine Implantation At the Surface Of A Realistic Device (Structure B)

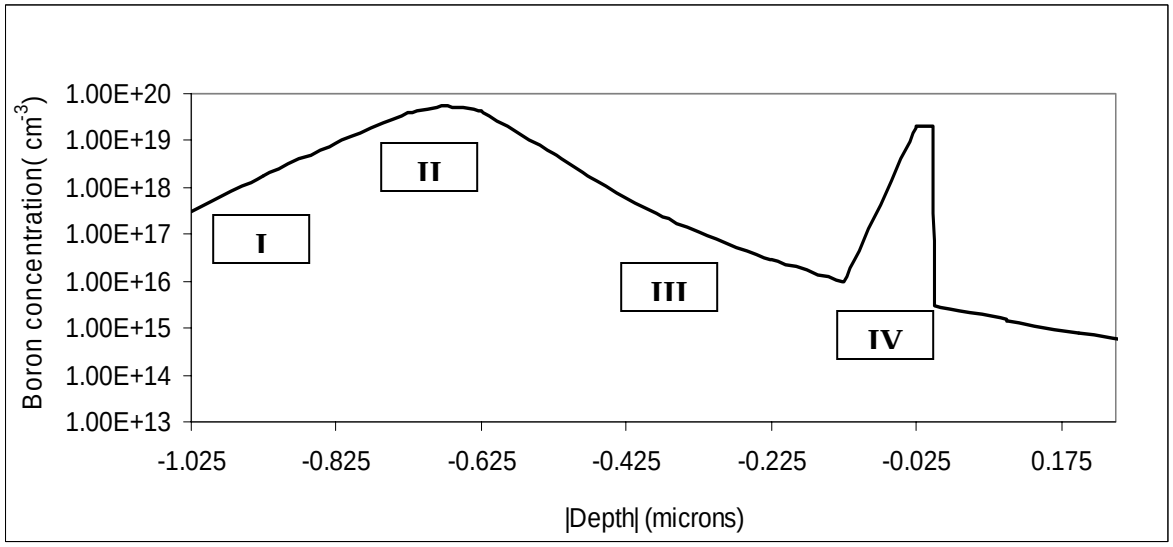

Figure 4.12: Boron concentration before diffusion for 120 keV implantation energy, dose 2 x $10^{19}/cm^3$ boron implantation (without diffusion)

The following figure 4.12 to figure 4.21 are obtained for the structure B which is important to observer the ion projection based on different opening. Generally all the graphs shows the same trend as companied to figure 4.1 to 4.9 for structure A. However it is observed that there are slightly difference concentrations as well as vacancies concentration. The differences are caused by the differences of ion trajectories during implantation process based on different opening.

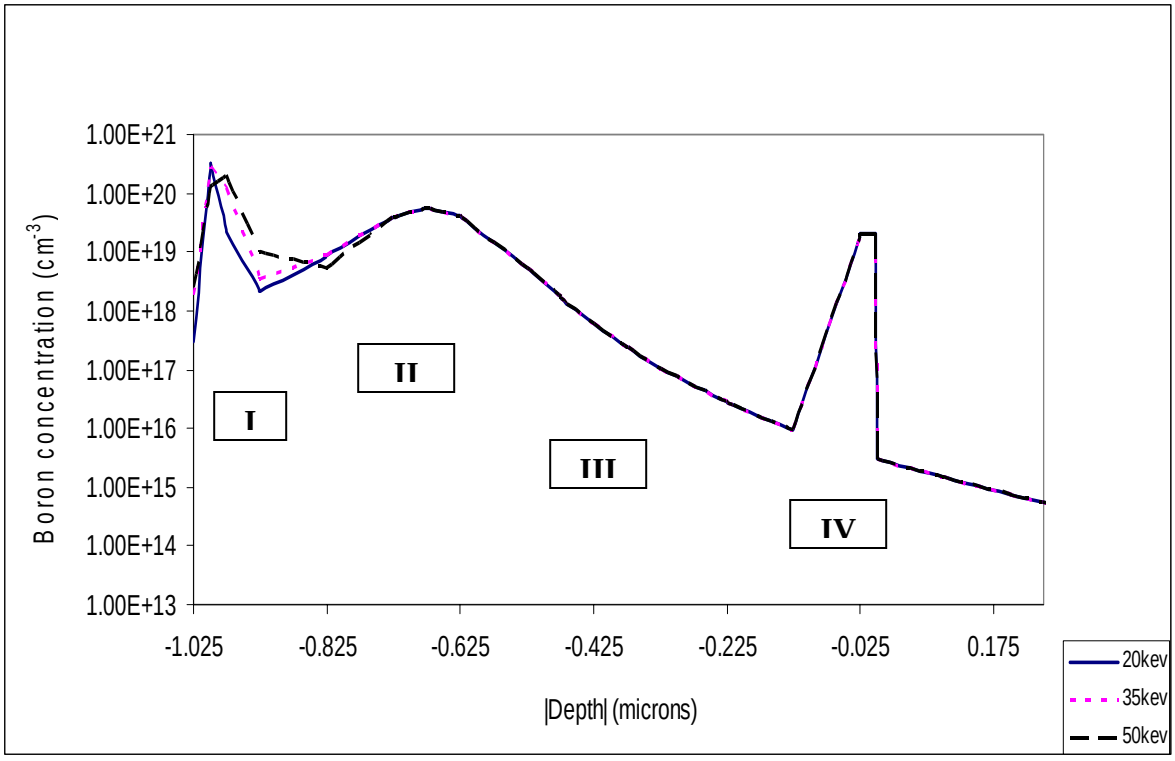

Figure 4.13: Different boron concentration of 120 keV boron implanted followed by 20 keV, 35 keV and 50 keV BF_2^+ implantation before diffusion

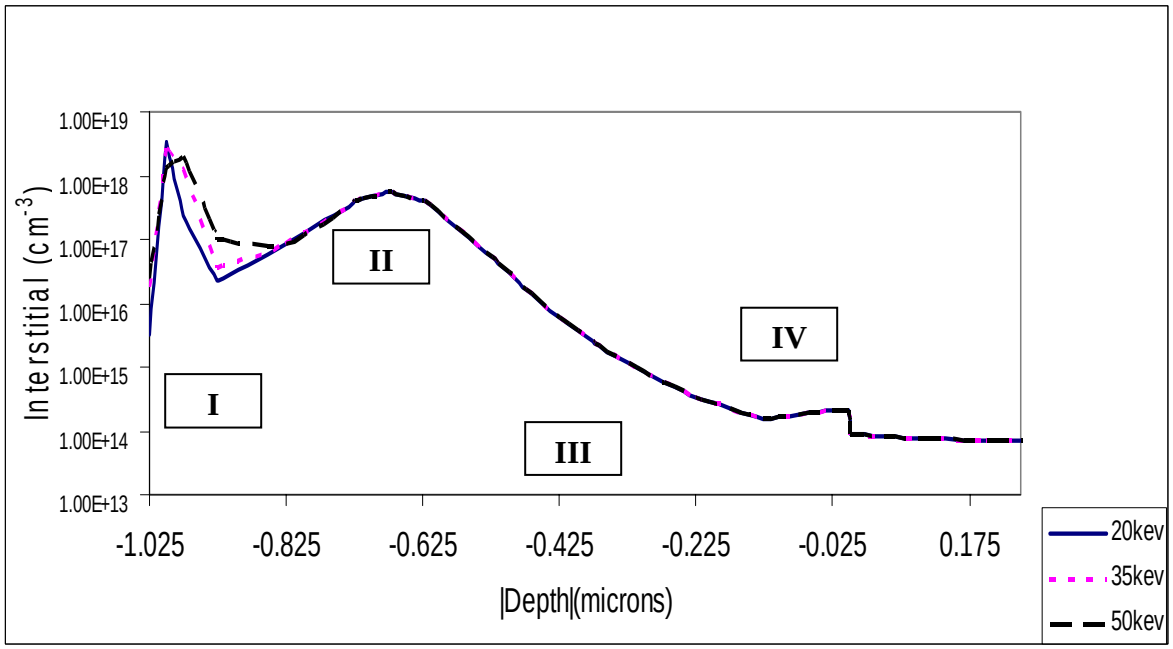

Figure 4.14: Different boron interstitial concentration for 120 keV implanted boron, dose of 2 x $10^{19}/cm^3$ followed by 20, 35 and 50 keV BF_2^+ implantation before diffusion

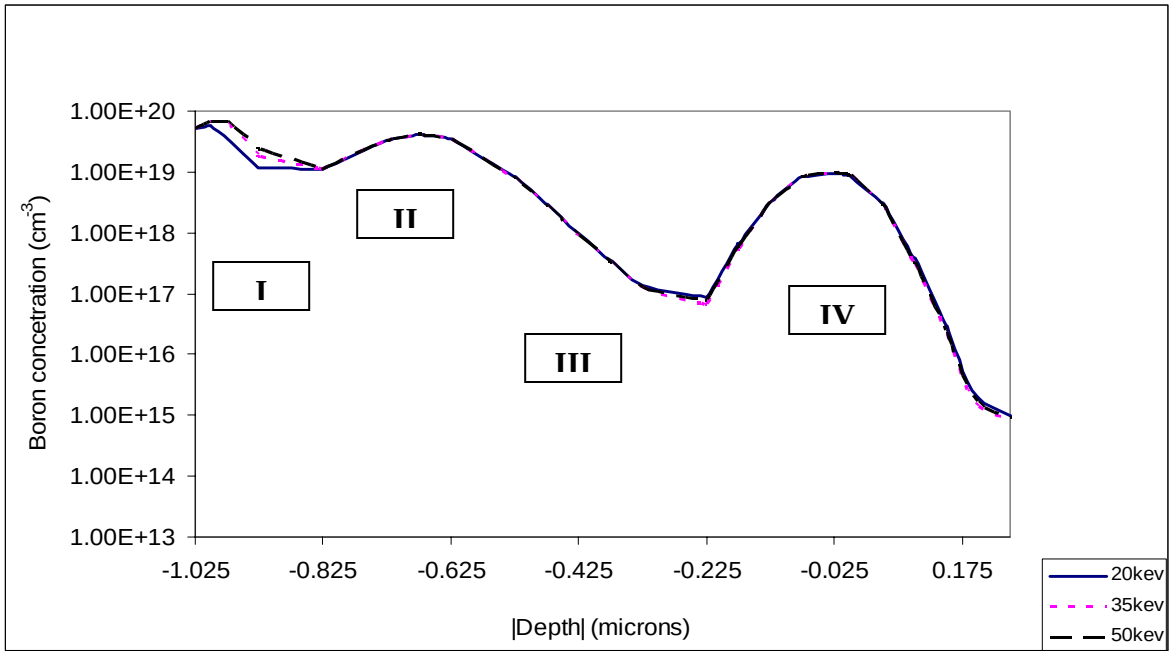

Figure 4.15: Different boron concentration of 120 keV boron implanted follow by 20 keV, 35 keV and 50 keV BF_2^+ implantation after diffusion

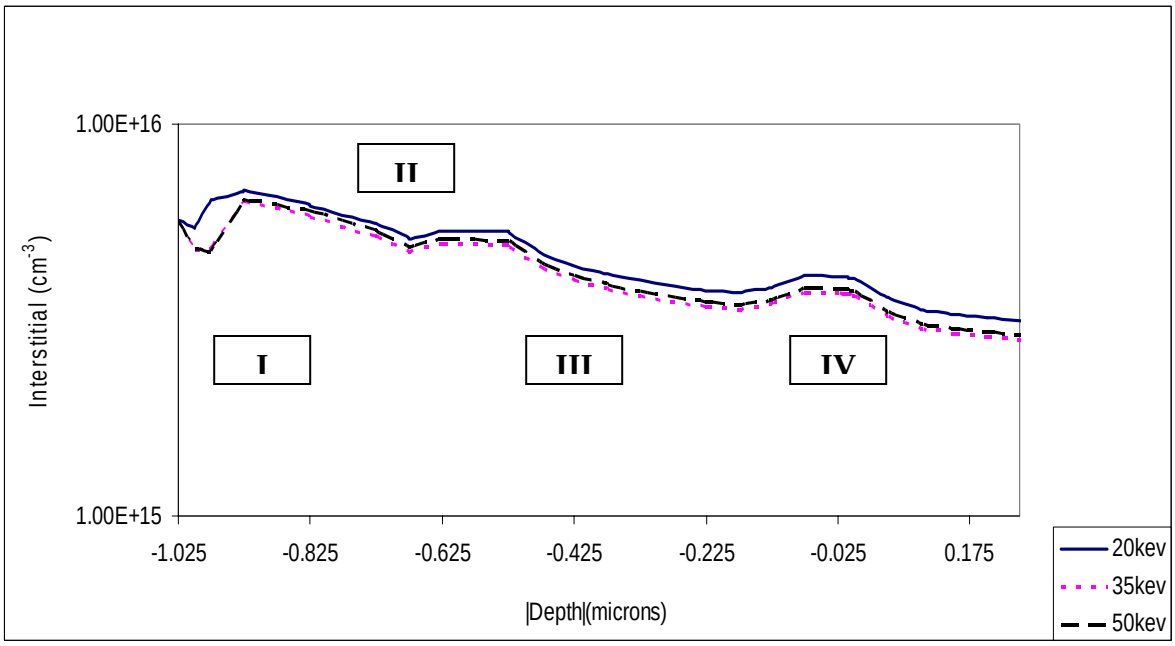

Figure 4.16: Different boron interstitial concentration for 120 keV implanted boron, dose of 2 x $10^{19}/cm^3$ followed by 20, 35 and 50 keV BF_2^+ implantation after diffusion

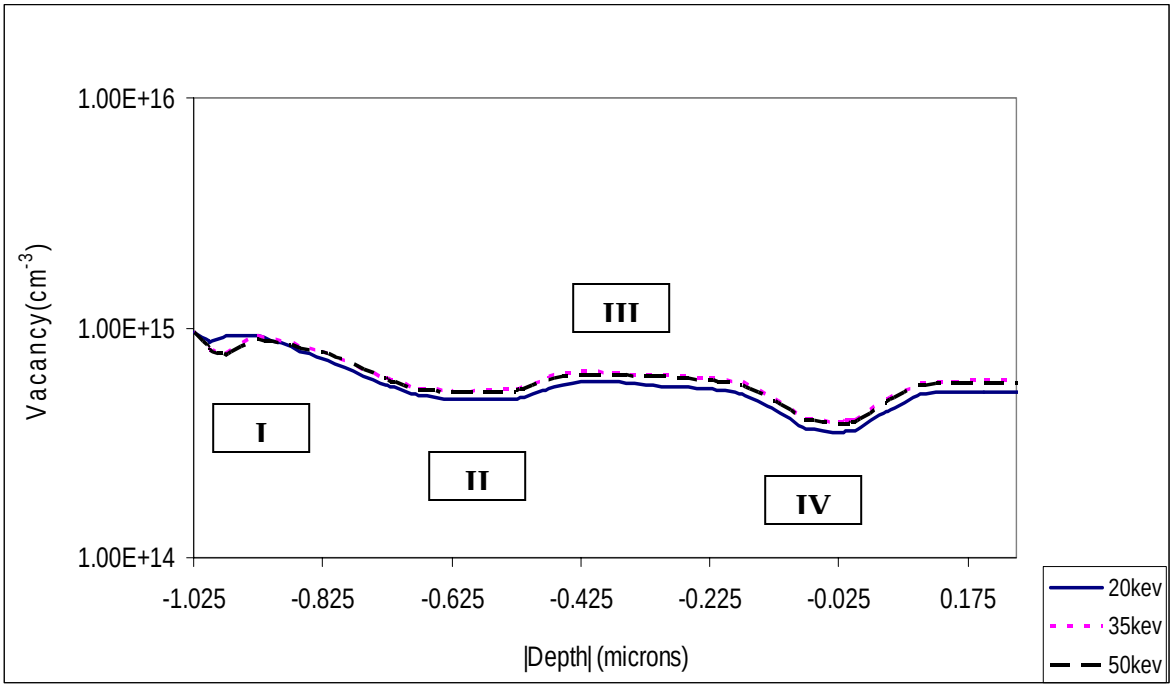

Figure 4.17: Different boron vacancy concentration for 120 keV implanted boron, dose of 2 x $10^{19}/cm^3$ followed by 20, 35 and 50 keV BF_2^+ implantation after diffusion

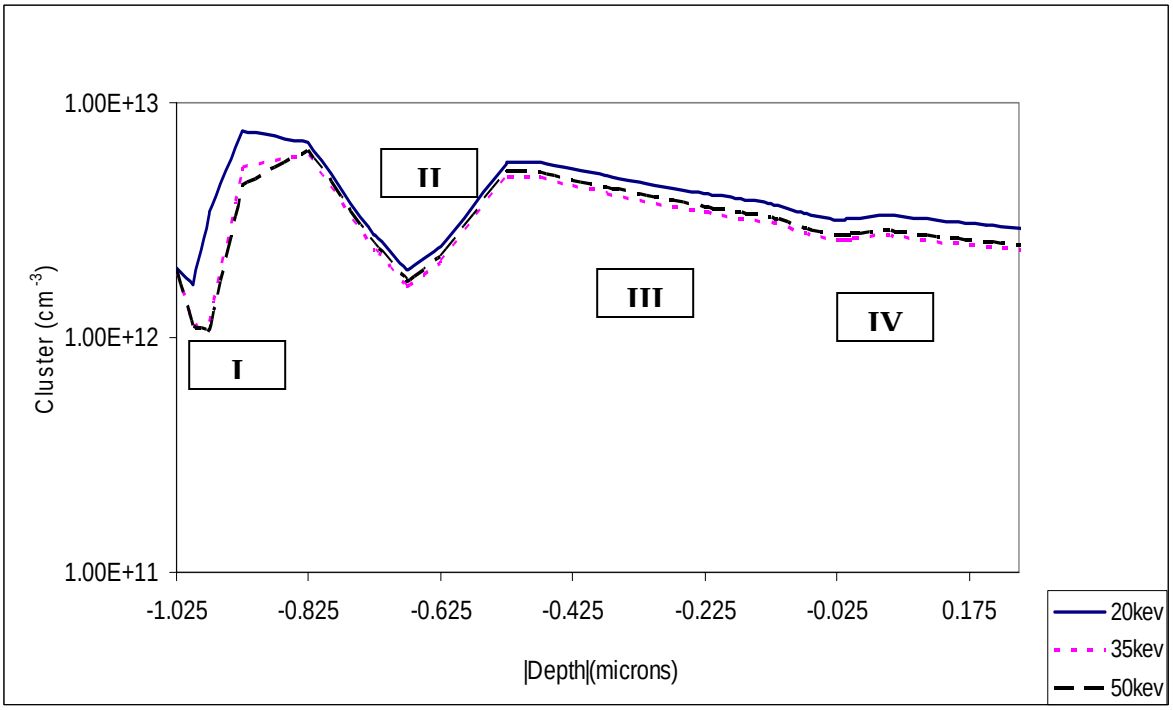

Figure 4.18: Different cluster interstitial concentration for 120 keV implanted boron, dose of 2 x $10^{19}/cm^3$ followed by 20, 35 and 50 keV BF_2^+ implantation after diffusion

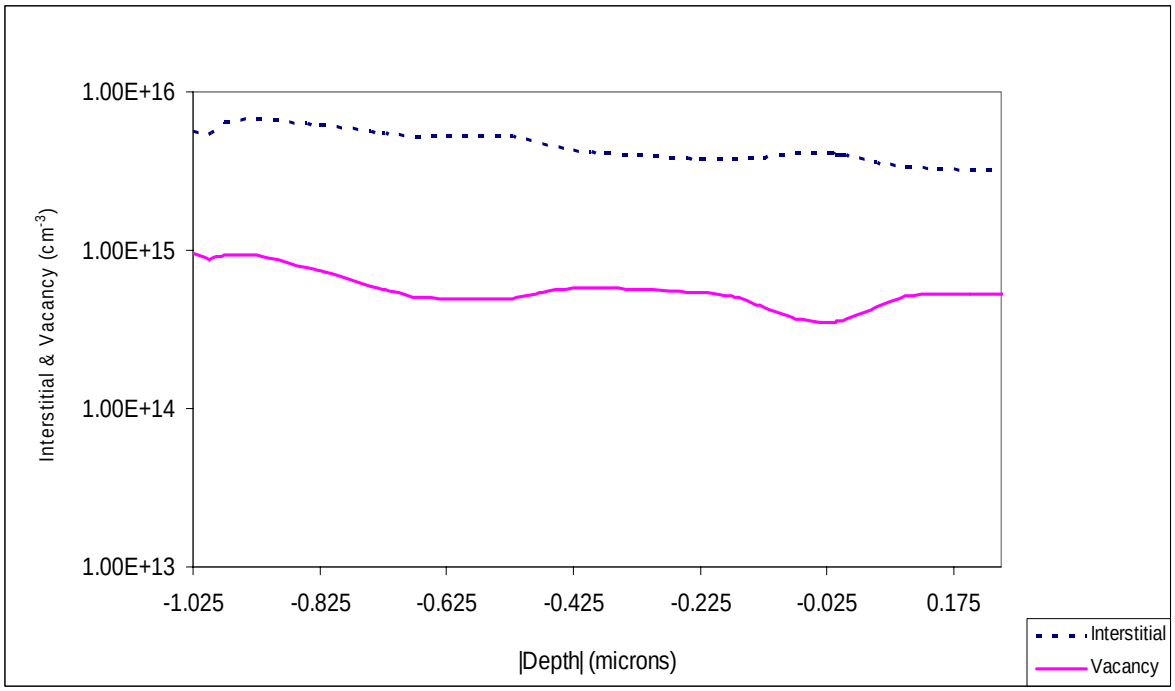

Figure 4.19: Interstitial and vacancy concentration for 120 keV implanted boron, dose of 2 x $10^{19}/cm^3$ followed by 20 keV BF_2^+ implantation after diffusion

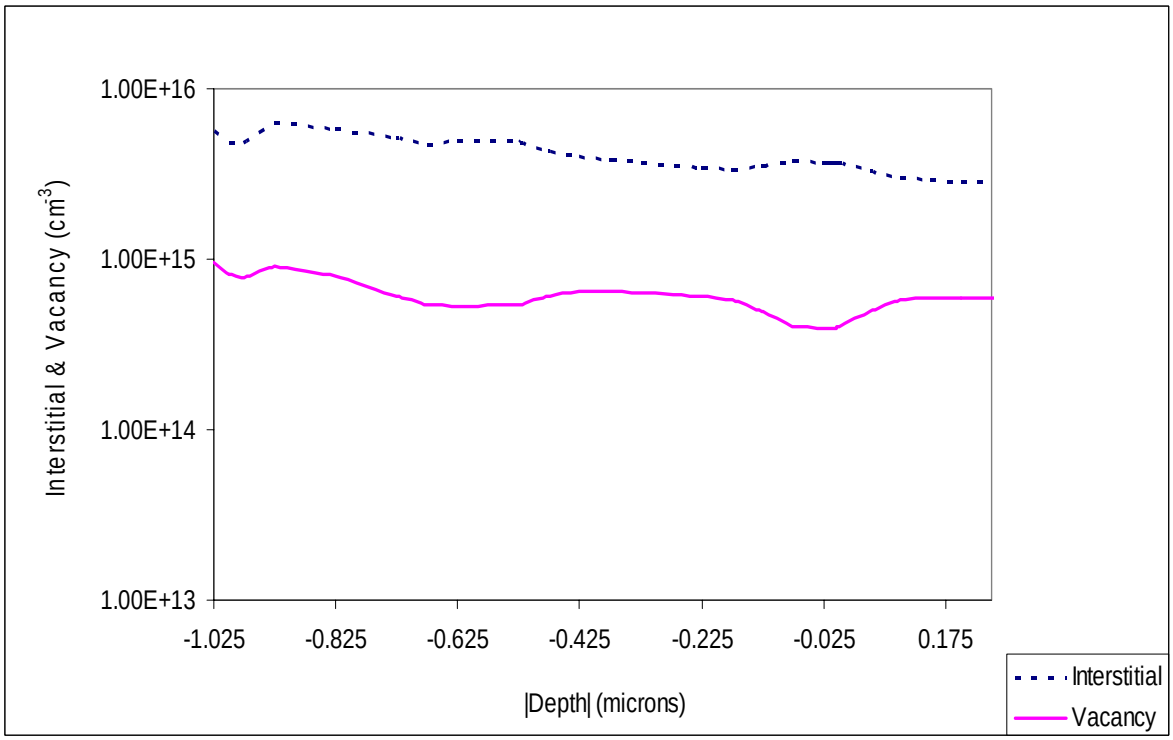

Figure 4.20: Interstitial and vacancy concentration for 120 keV implanted boron, dose of 2 x $10^{19}/cm^3$ followed by 35 keV BF_2^+ implantation after diffusion

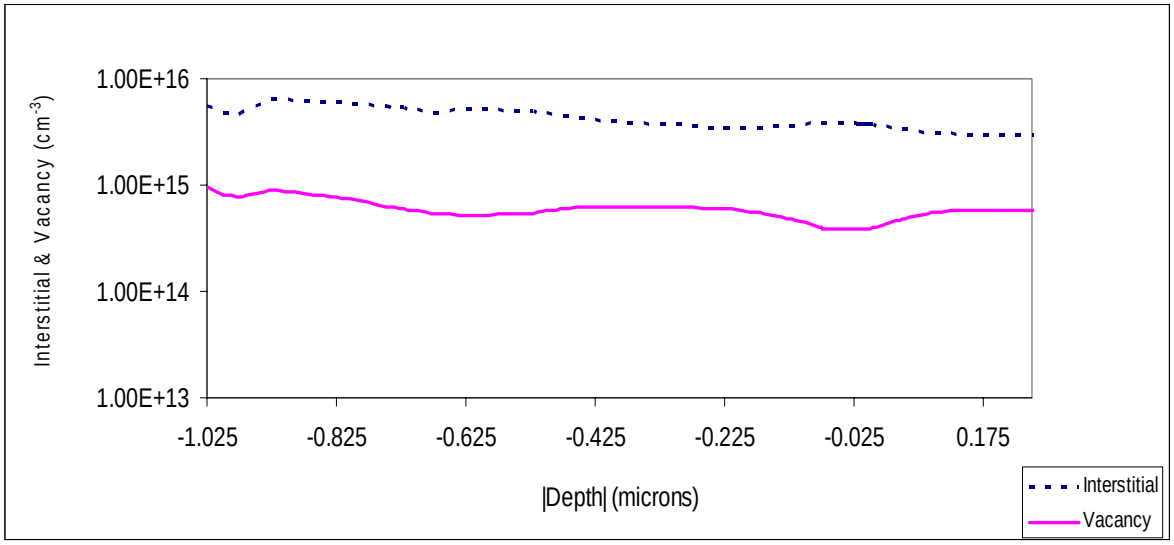

Figure 4.21: Interstitial and vacancy concentration for 120 keV implanted boron, dose of 2 x $10^{19}/cm^3$ followed by 50 keV BF_2^+ implantation after diffusion

4.3 Fluorine Implantation At the Surface Of A Realistic Device (Structure B)

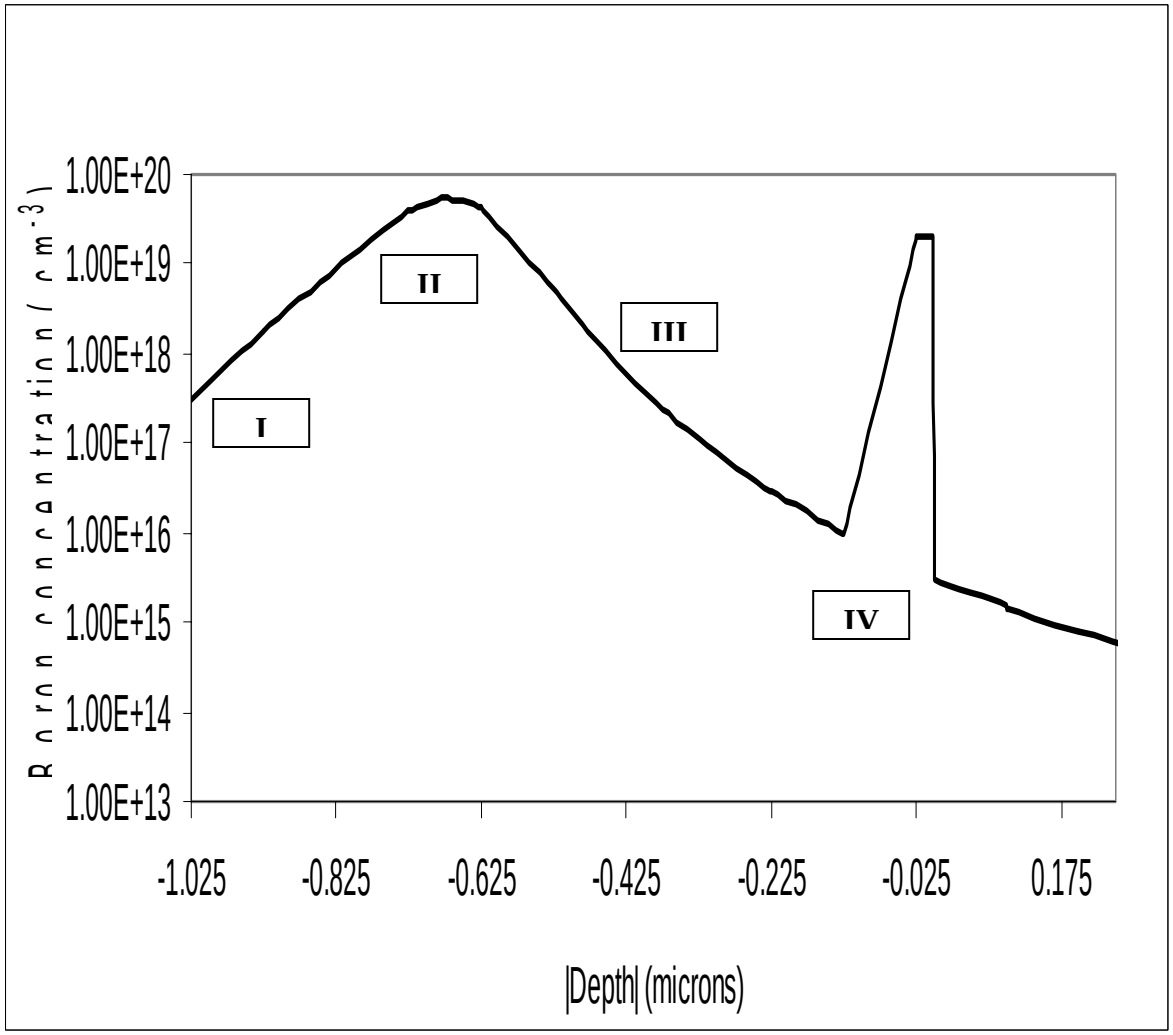

Figure 4.12: Boron concentration before diffusion for 120 kev energy, dose 2 x $10^{19}/cm^3$ boron implantation

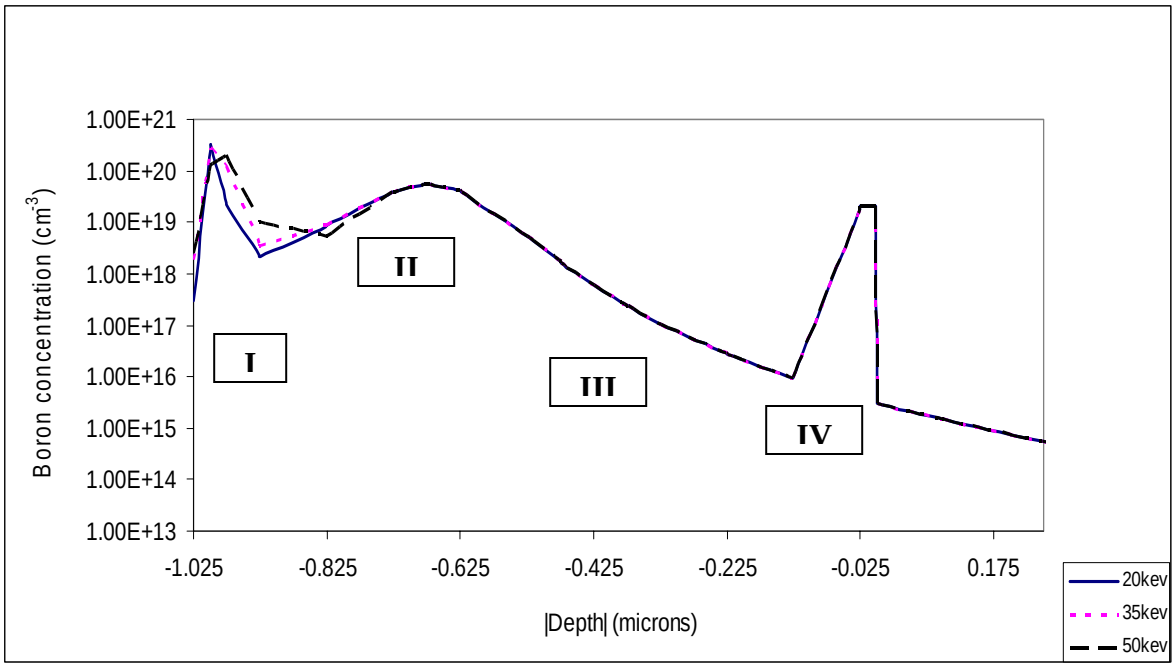

Figure 4.13: Different boron concentration of 120 kev boron implanted follow by 20 kev, 35 kev and 50 kev BF_2^+ implantation before diffusion

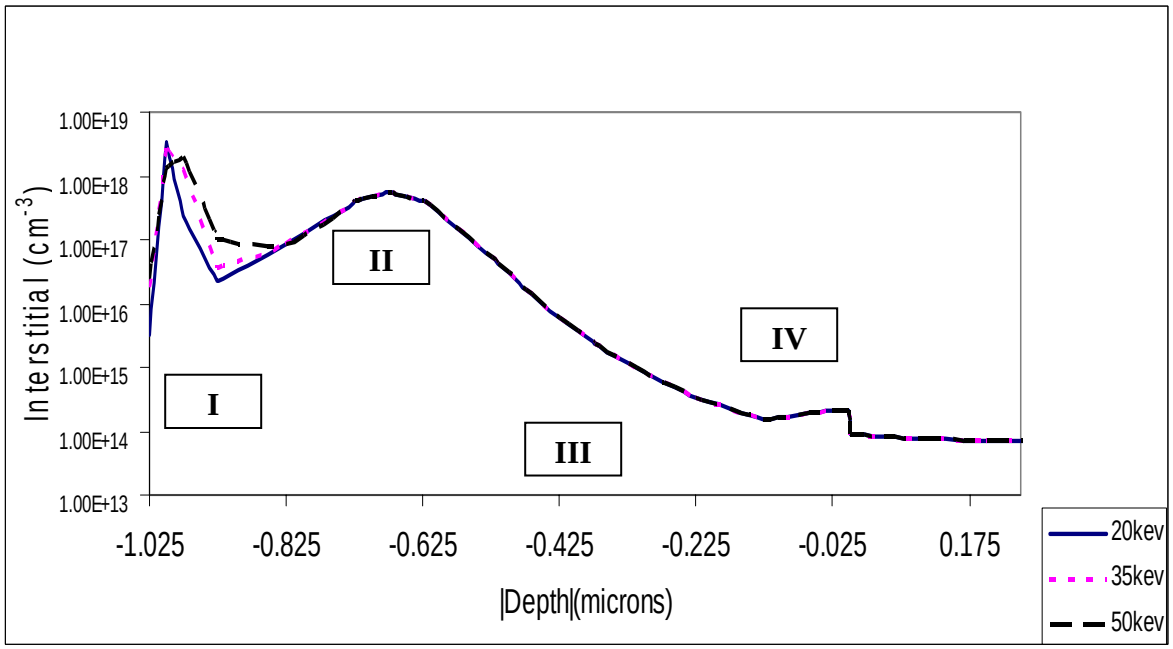

Figure 4.14: Different boron interstitial concentration for 120 kev implanted boron, dose of 2 x $10^{19}/cm^3$ followed by 20, 35 and 50 kev BF_2^+ implantation before diffusion

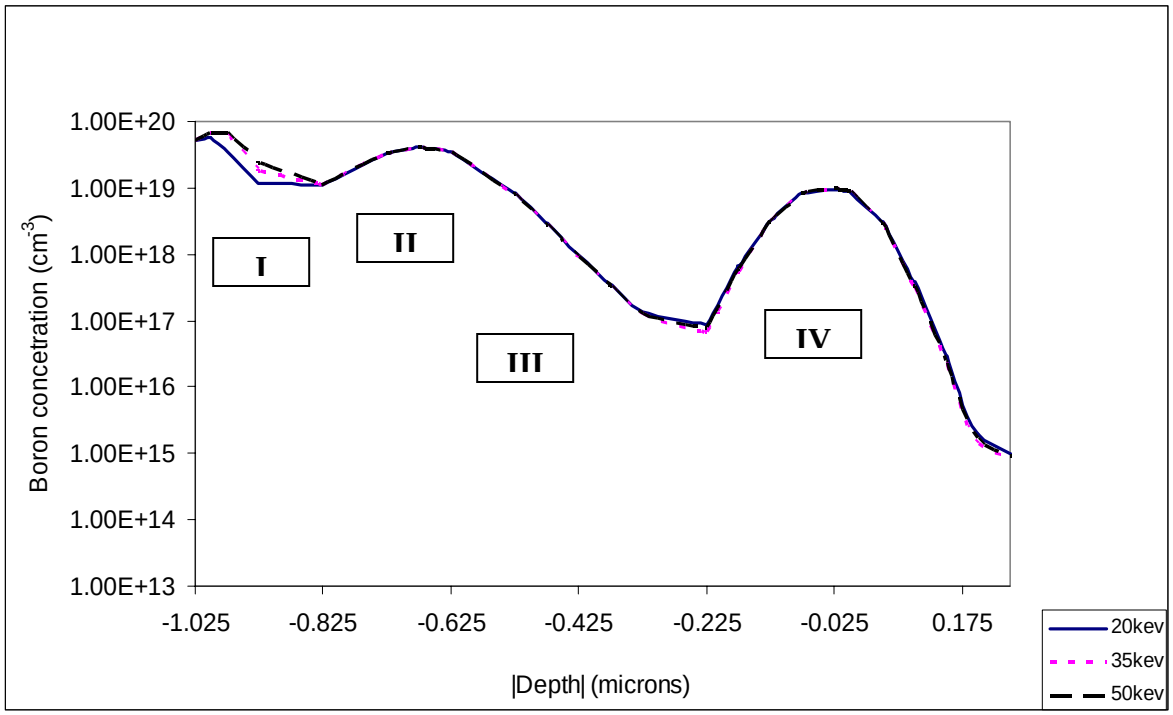

Figure 4.15: Different boron concentration of 120 kev boron implanted follow by 20 kev, 35 kev and 50 kev BF_2^+ implantation after diffusion

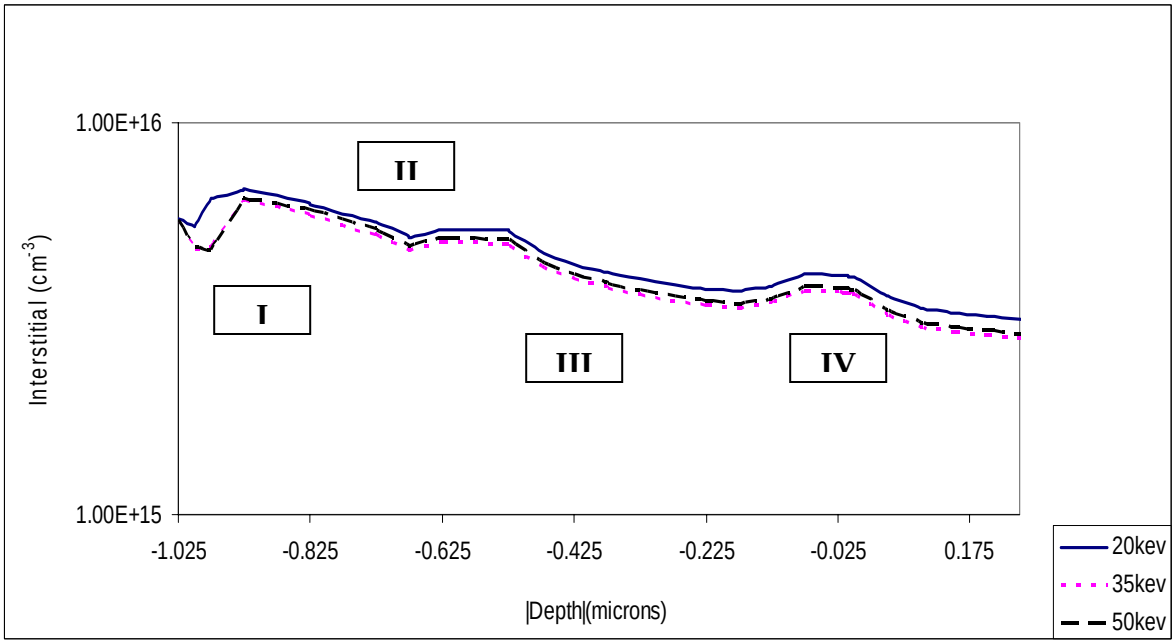

Figure 4.16: Different boron interstitial concentration for 120 kev implanted boron, dose of 2 x $10^{19}/cm^3$ followed by 20, 35 and 50 kev BF_2^+ implantation after diffusion

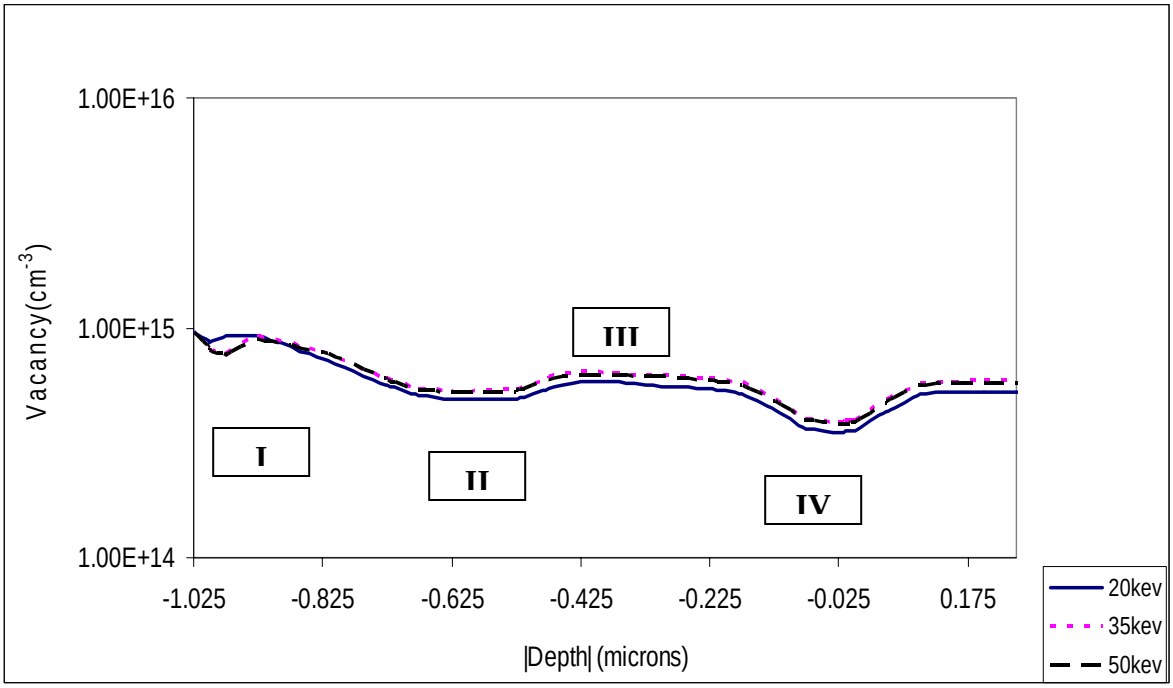

Figure 4.17: Different boron vacancy concentration for 120 kev implanted boron, dose of 2 x $10^{19}/cm^3$ followed by 20, 35 and 50 kev BF_2^+ implantation after diffusion

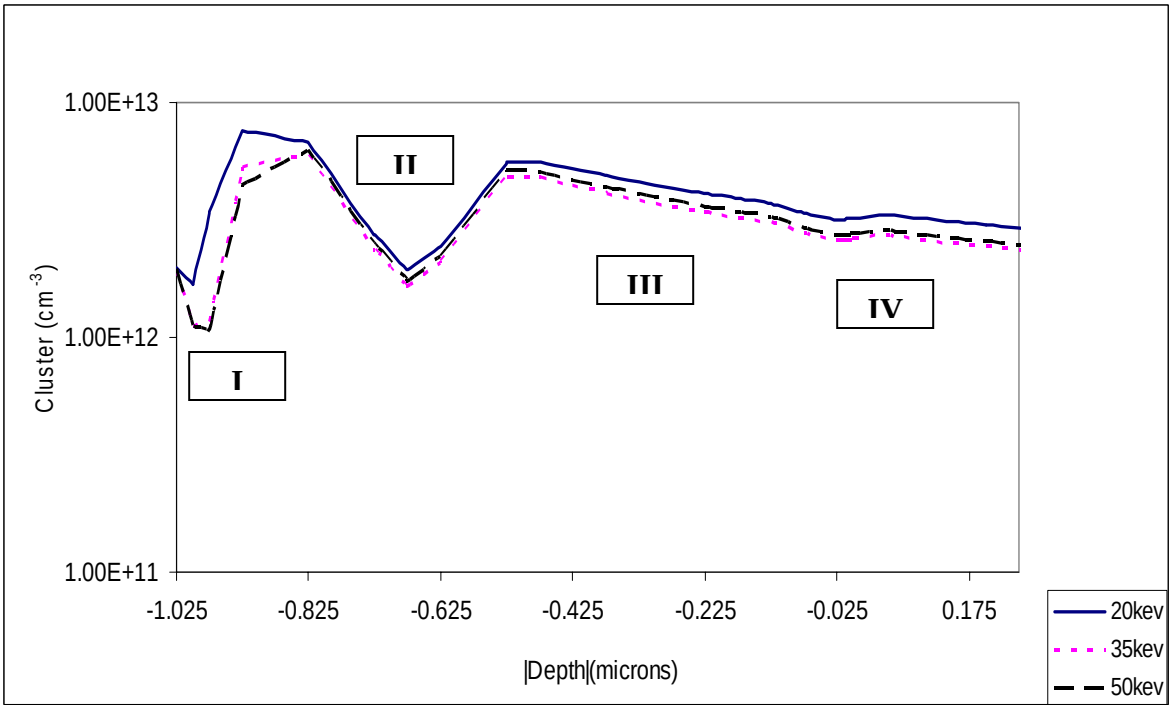

Figure 4.18: Different cluster interstitial concentration for 120 kev implanted boron, dose of 2 x $10^{19}/cm^3$ followed by 20, 35 and 50 kev BF_2^+ implantation after diffusion

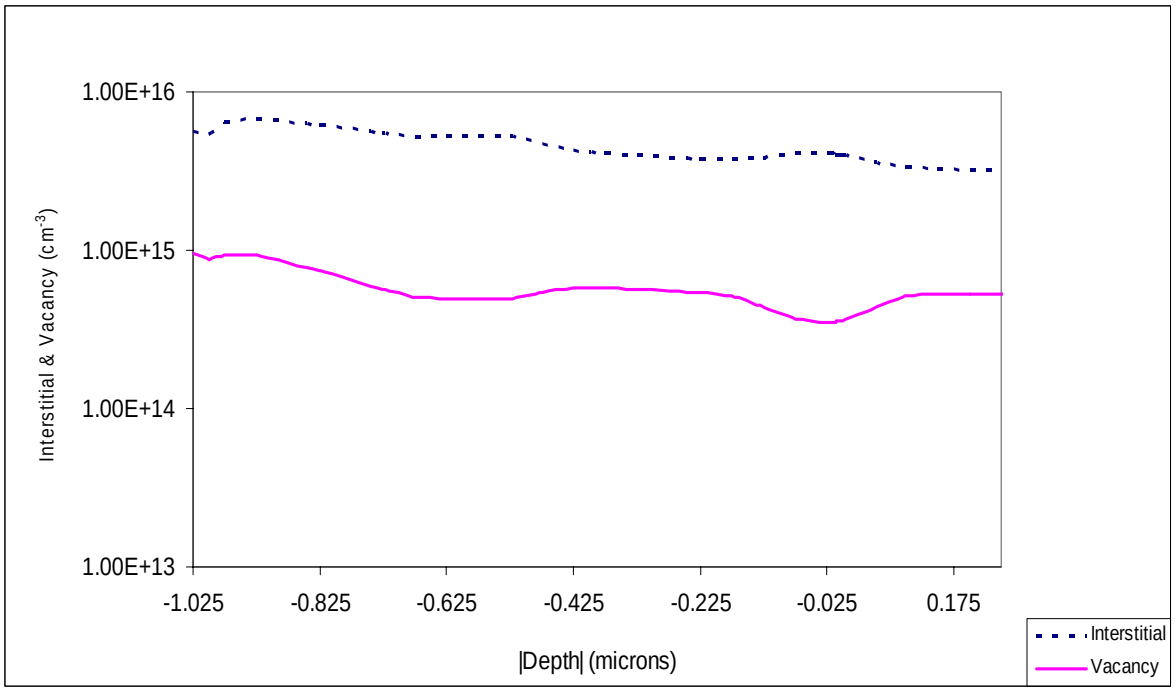

Figure 4.19: Interstitial and vacancy concentration for 120 kev implanted boron, dose of 2 x $10^{19}/cm^3$ followed by 20 kev BF_2^+ implantation after diffusion

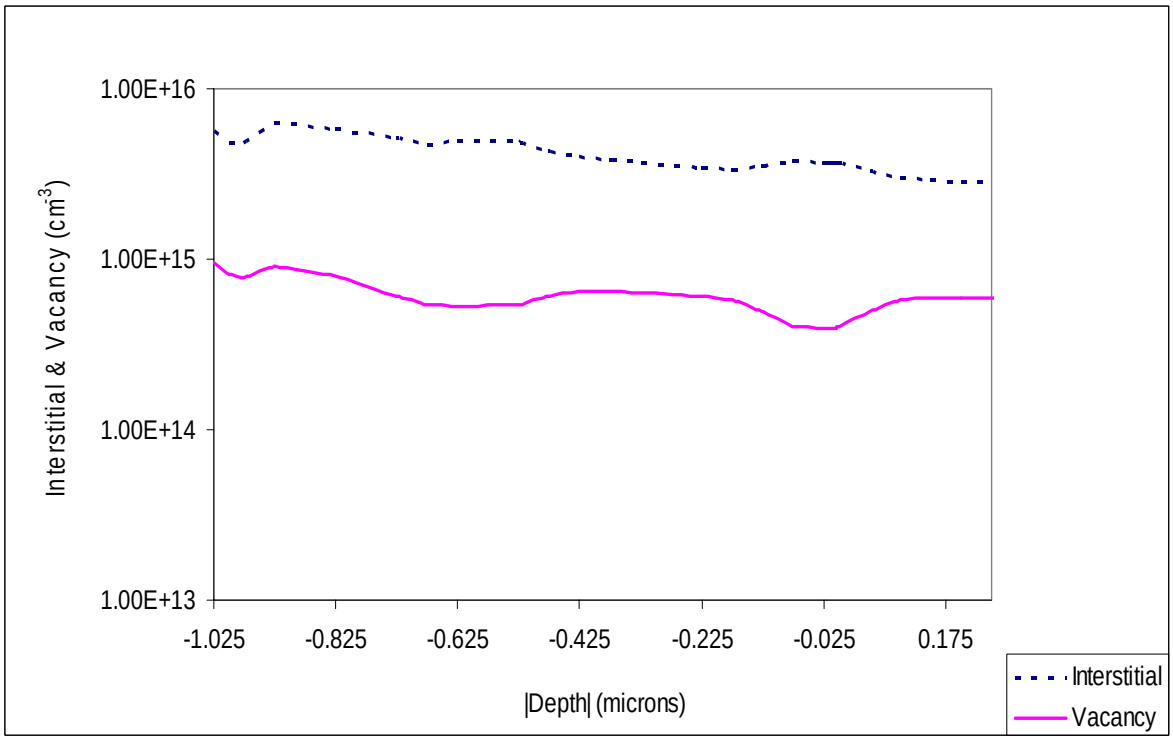

Figure 4.20: Interstitial and vacancy concentration for 120 kev implanted boron, dose of 2 x $10^{19}/cm^3$ followed by 35 kev BF_2^+ implantation after diffusion

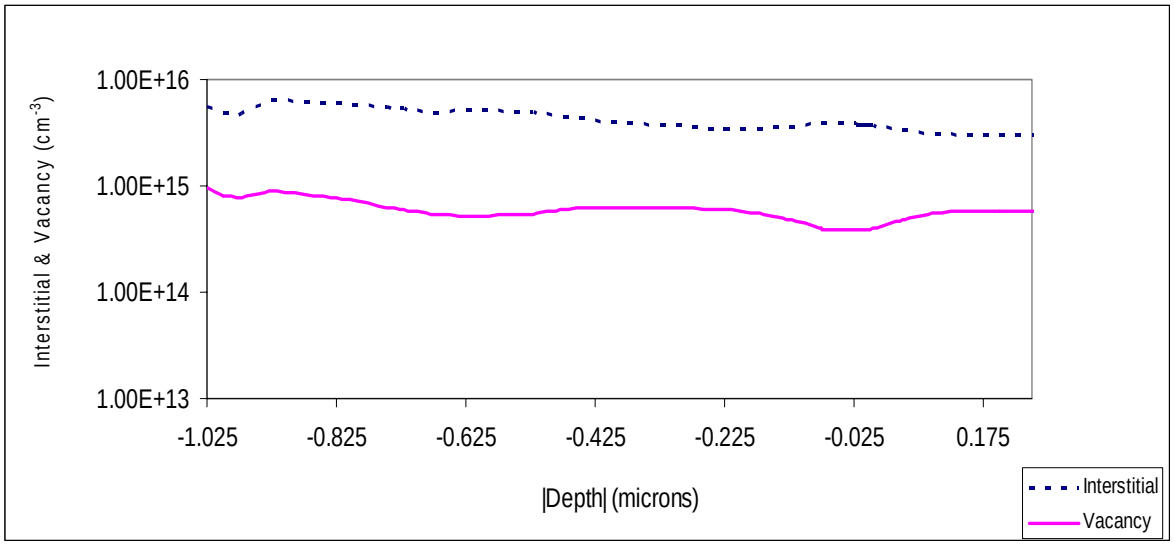

Figure 4.21: Interstitial and vacancy concentration for 120 kev implanted boron, dose of 2 x $10^{19}/cm^3$ followed by 50 kev BF_2^+ implantation after diffusion

Figure 4.12 show the boron concentration before diffusion for 120 kev energy, dose 2 x $10^{19}/cm^3$ boron implantation. The structure B in this project is used for comparing the channelling effect and the ion projected. The structure of structure B is show in the chapter 3 methodology. By observed form the figure 4.12, comparing the result from structure A figure 4.0, the underlying layer have quite different. The underlying layer for structure B seems looks narrow than the structure A. The boron concentration for the structure A is a little bit higher than the structure B. It is because the structure B's design had block some of the implantation energy compare with the structure.

The phenomenon and the explanations for interstitial, vacancies cluster and boron concentration between the structure A and structure B is same. The main focusing of this project is in structure A.